

Above-threshold ionization of hydrogen atom in chirped laser fields

Yuan-Yuan Ni(倪园园), Song-Feng Zhao(赵松峰), Xiao-Yong Li(李小勇), Guo-Li Wang(王国利), Xiao-Xin Zhou(周效信)

Citation: Chin. Phys. B . 2018, 27(7): 073203. **doi:** 10.1088/1674-1056/27/7/073203

Journal homepage: http://cpb.iphy.ac.cn; http://iopscience.iop.org/cpb

What follows is a list of articles you may be interested in

Dynamic stabilization of Na atom in an intense pulsed laser field

Xiao-Li Guo(郭晓丽), Song-Feng Zhao(赵松峰), Guo-Li Wang(王国利), Xiao-Xin Zhou(周效信)

Chin. Phys. B . 2018, 27(4): 043201. **doi:** 10.1088/1674-1056/27/4/043201

Semiclassical investigation of Coulomb focusing effects in atomic above-threshold ionization with elliptically polarized laser fields

Chuan-Liang Wang(王传亮), Li-Xin Xia(夏立新), Hong-Bin Yao(姚洪斌), Wen-Liang Li(李文亮)

Chin. Phys. B . 2017, 26(4): 043201. **doi:** 10.1088/1674-1056/26/4/043201

Dependence of above-threshold ionization spectrum on polarization directions of two-color laser fields

Liu Min, Guo Ying-Chun, Wang Bing-Bing

Chin. Phys. B . 2015, 24(7): 073201. **doi:** 10.1088/1674-1056/24/7/073201

Influence of multi-photon excitation on the atomic above-threshold ionization

Tian Yuan-Ye, Wang Chun-Cheng, Li Su-Yu, Guo Fu-Ming, Ding Da-Jun, Roeterdink Wim-G, Chen Ji-Gen, Zeng Si-Liang, Liu Xue-Shen, Yang Yu-Jun

Chin. Phys. B . 2015, 24(4): 043202. **doi:** 10.1088/1674-1056/24/4/043202

The Coulomb effect on a low-energy structure in above-threshold ionization spectra induced by mid-infrared laser pulses

Lin Zhi-Yang, Wu Ming-Yan, Quan Wei, Liu Xiao-Jun, Chen Jing, Cheng Ya

Chin. Phys. B . 2014, 23(2): 023201. **doi:** 10.1088/1674-1056/23/2/023201

Above-threshold ionization of hydrogen atom in chirped laser fields*

Yuan-Yuan Ni(倪园园)[1], Song-Feng Zhao(赵松峰)[1,†], Xiao-Yong Li(李小勇)[2], Guo-Li Wang(王国利)[1], and Xiao-Xin Zhou(周效信)[1]

[1] *Key Laboratory of Atomic and Molecular Physics and Functional Materials of Gansu Province, College of Physics and Electronic Engineering, Northwest Normal University, Lanzhou* 730070, *China*
[2] *Experimental Center, Northwest University for Nationalities, Lanzhou* 730030, *China*

(Received 12 March 2018; revised manuscript received 13 April 2018; published online 25 June 2018)

Above-threshold ionization (ATI) of a hydrogen atom exposed to chirped laser fields is investigated theoretically by solving the time-dependent Schrödinger equation. By comparing the energy spectra, the two-dimensional momentum spectra, and the angular distributions of photoelectron for the laser pulses with different chirp rates, we show a very clear chirp dependence both in the multiphoton and tunneling ionization processes but no chirp dependence in the single-photon ionization. We find that the chirp dependence in the multiphoton ionization based ATI can be attributed to the excited bound states. In the single-photon and tunneling ionization regimes, the electron can be removed directly from the ground state and thus the excited states may not be very important. It indicates that the chirp dependence in the tunneling ionization based ATI processes is mainly due to the laser pulses with different chirp rates.

Keywords: above-threshold ionization, chirped laser field, time-dependent Schrödinger equation

PACS: 32.80.Rm, 42.50.Hz **DOI:** 10.1088/1674-1056/27/7/073203

1. Introduction

Above-threshold ionization (ATI) of atoms by the transform-limited (i.e., chirp-free) laser pulses has been widely investigated both experimentally[1–8] and theoretically.[9–15] However, there is less attention paid to the ATI of atoms in chirped laser pulses. Wang *et al.*[16] reported experimentally the chirp dependence of Freeman resonance structures in the ATI spectra of Xe exposed to chirped intense laser pulses. Theoretically, Nakajima *et al.*[17] investigated the ATI of Na by chirped infrared laser pulses by solving the three-dimensional time-dependent Schrödinger equation (3D-TDSE) and attributed the chirp dependence of the photoelectron angular distributions (PADs) to the excited bound states in the multiphoton ionization processes. Laulan *et al.*[18] studied excitation and ionization of hydrogen atoms in intense chirped laser pulses. Xiang *et al.*[19] found that the cutoff of the ATI of one-dimensional H atoms can be extended dramatically using a few-cycle nonlinear chirped laser pulse. Peng *et al.*[20,21] analyzed numerically how the asymmetry parameters of the ionized electron momentum distributions of the H atom depend on the chirp rate of the few-cycle attosecond pulses in the single-photon ionization region. Pronin *et al.*[22] explained the chirp dependence of the asymmetry in the ionized electron distributions of atoms by a chirped few-cycle attosecond pulse with the perturbation theory. Furthermore, chirped laser pulses have also been applied extensively in quantum control study[23] and the coherent control of high-order harmonics and attosecond pulse duration.[24–29]

Mechanically, the electrons in atoms exposed to an intense laser field can be released into a continuum state by absorbing a single high-energy photon, absorbing simultaneously several photons, or tunneling through the potential barrier formed by the Coulomb force and the laser field. According to the Keldysh theory,[30] these different ionization mechanisms can be distinguished by the Keldysh parameter $\gamma = \sqrt{I_{\rm p}/2U_{\rm p}}$, where $I_{\rm p}$ is the ionization potential and $U_{\rm p}$ is the ponderomotive energy. So far, most efforts have been paid to the ATI of atoms and molecules by chirped laser fields in the single-photon ionization and multiphoton ionization regimes, and the question concerning the chirp effect on the ATI in the tunneling ionization regime still remains open.

In this paper, we theoretically investigate how the chirp rate of the laser pulses affects the energy spectra, the two-dimensional (2D) momentum spectra, and the PADs of the H atom in the single-photon, multiphoton, and tunneling ionization processes by solving the TDSE. The rest of this paper is arranged as follows. In Section 2, we briefly describe how to calculate the energy spectra and the 2D momentum spectra of the H atom in chirped laser fields by solving the TDSE. In Section 3, we present the chirp dependence of the energy spectra, the PADs, and the 2D electron momentum spectra of the H atom in the single-photon, multiphoton, and tunneling ionization regimes. A conclusion will be given in Section 4. Atomic units are used throughout this paper unless otherwise stated.

*Project supported by the National Natural Science Foundation of China (Grant Nos. 11664035, 11465016, 11764038, 11364038, and 11564033).
†Corresponding author. E-mail: zhaosf@nwnu.edu.cn
© 2018 Chinese Physical Society and IOP Publishing Ltd

2. Theory and method

Under the dipole approximation and the length gauge, the TDSE of the H atom in the presence of a linearly polarized laser field can be written as

$$\begin{aligned} \mathrm{i}\frac{\partial}{\partial t}\Psi(\boldsymbol{r},t) &= [H_0+H_{\mathrm{i}}(t)]\Psi(\boldsymbol{r},t) \\ &= \left[-\frac{1}{2}\nabla^2-\frac{1}{r}+H_{\mathrm{i}}(t)\right]\Psi(\boldsymbol{r},t). \end{aligned} \tag{1}$$

Here, H_0 is the field-free atomic Hamiltonian and the atom–field interaction $H_{\mathrm{i}}(t)$ is given by

$$H_{\mathrm{i}}(t)=\boldsymbol{r}\cdot\boldsymbol{E}(t), \tag{2}$$

where $\boldsymbol{E}(t)$ is the laser's electric field. The time-dependent wave function $\Psi(\boldsymbol{r},t)$ is expanded as

$$\Psi(\boldsymbol{r},t)=\sum_{nl}C_{nl}(t)R_{nl}(r)Y_{lm}(\hat{\boldsymbol{r}}), \tag{3}$$

where $R_{nl}(r)Y_{lm}(\hat{\boldsymbol{r}})$ is the eigenfunction of H_0 within the box of $r\in[0,r_{\max}]$, and $R_{nl}(r)$ and $Y_{lm}(\hat{\boldsymbol{r}})$ are expanded by the discrete variable representation (DVR) basis sets[31–33] associated with Legendre polynomials, while $C_{nl}(t)$ is obtained by using the split-operator method.[34] The total population distribution of the excited states is calculated by

$$P_{\mathrm{ex}}(t)=\sum_{n'l'}|C_{n'l'}(t)|^2. \tag{4}$$

Here $n'l'$ runs over all excited bound states. In this paper, we typically take $r_{\max}=2000$ a.u. and $l_{\max}=120$.

The PADs and the 2D momentum spectra are obtained by projecting the final wave function at the end of the pulse onto eigenstates of a continuum electron $\Phi_{\boldsymbol{p}}^-$ with a given momentum vector $\boldsymbol{p}$,

$$P_1(E,\theta)=\frac{\partial^2 P}{\partial E\partial\theta}=\left|\langle\Phi_{\boldsymbol{p}}^-|\Psi(\boldsymbol{r},t=t_{\mathrm{f}})\rangle\right|^2 2\pi p\sin\theta, \tag{5}$$

where $E=p^2/2$ is the kinetic energy of the photoelectron and θ is the angle between the emission direction of the ejected photoelectron and the polarization axis of the laser field. The continuum state $\Phi_{\boldsymbol{p}}^-$ satisfies the following equation:

$$\left(-\frac{1}{2}\nabla^2-\frac{1}{r}\right)\Phi_{\boldsymbol{p}}^-=E\Phi_{\boldsymbol{p}}^-. \tag{6}$$

By integrating over θ in Eq. (5), we obtain the photoelectron energy spectra

$$\frac{\partial P}{\partial E}=\int\frac{\partial^2 P}{\partial E\partial\theta}\,\mathrm{d}\theta. \tag{7}$$

In this paper, we consider a chirped femtosecond laser pulse having a Gaussian form, which is similar to that used in Refs. [17], [20], [21], and [35]. The laser pulse is assumed to be linearly polarized along the z axis with its vector potential given by

$$\boldsymbol{A}(t)=AF(t)\sin[\omega(t)t+\phi_0]\boldsymbol{e}_z, \tag{8}$$

where ϕ_0 is the carrier-envelope phase (CEP) of the laser pulse. The peak amplitude A, chirped carrier frequency $\omega(t)$, and time envelope $F(t)$ are given respectively by

$$A=\frac{E}{\omega_0}=\frac{1}{\omega_0}\sqrt{\frac{I_0/I_{\mathrm{au}}}{\sqrt{1+\xi^2}}}, \tag{9}$$

$$\omega(t)=\omega_0+4\ln 2\frac{\xi}{1+\xi^2}\frac{t}{\tau_0^2}, \tag{10}$$

$$F(t)=\exp\left(-4\ln 2\frac{1}{1+\xi^2}\frac{t^2}{\tau_0^2}\right). \tag{11}$$

Here, $I_{\mathrm{au}}=3.51\times10^{16}$ W/cm^2 and the parameter ξ is the chirp rate. The case $\xi=0$ corresponds to a transform-limited (i.e., chirp-free) pulse with carrier frequency ω_0, peak intensity I_0, and pulse duration τ_0 (full width at half maximum, FWHM). For a chirped pulse, the peak intensity and pulse duration are given by $I=I_0/\sqrt{1+\xi^2}$ and $\tau=\tau_0\sqrt{1+\xi^2}$, respectively. It is clear that a nonzero chirp ξ leads to a decrease in the peak intensity and an increase in the pulse duration for a fixed total pulse energy. The electric field strength of the laser pulse is given by the time derivative of the vector potential, i.e., $\boldsymbol{E}(t)=-\partial\boldsymbol{A}(t)/\partial t$.

3. Numerical results and discussion

3.1. Check the reliability of present numerical calculations

In Ref. [36], we compared carefully the energy spectra and the 2D momentum distributions of H obtained from the TDSE based on the length and the velocity gauges, respectively. To further check the reliability of our numerical

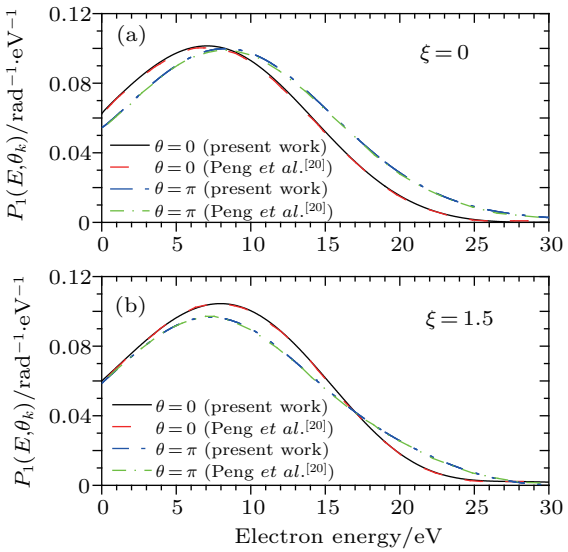


Fig. 1. (color online) Differential probabilities $P_1(E,\theta_k)$ of electrons ionized along $\theta=0$ and $\theta=\pi$ for (a) $\xi=0$ and (b) $\xi=1.5$. The transform-limited laser pulse has central carrier frequency $\omega_0=25$ eV, CEP $\phi_0=0.5\pi$, intensity $I_0=1\times10^{15}$ W/cm^2, and duration $\tau_0=T_0=2\pi/\omega_0$.

simulations, in Fig. 1, we compare the present differential probabilities of electrons ionized along $\theta = 0$, π for two different chirp rates $\xi = 0$, 1.5 with those in Ref. [20]. The laser pulse for $\xi = 0$ has central carrier frequency $\omega_0 = 25$ eV, CEP $\phi_0 = 0.5\pi$, intensity $I_0 = 1 \times 10^{15}$ W/cm^2, and duration $\tau_0 = T_0 = 2\pi/\omega_0$. Clearly, the present differential probabilities agree perfectly with those documented in Ref. [20], which were obtained from the TDSE using the velocity gauge.

In the following, we show how the chirp rate of the laser pulses affects the PES, the PADs, and the 2D momentum spectra of the H atom in the multiphoton, single-photon, and tunneling ionization regimes, respectively. We take $\phi_0 = 0$ for all the numerical calculations in the rest of this paper.

3.2. Multiphoton ionization regime

In our simulations, we choose a $\tau_0 = 5$ fs (FWHM) laser field with the peak laser intensity of $I_0 = 1.3 \times 10^{13}$ W/cm^2 and central wavelength $\lambda_0 = 400$ nm for the transform-limited pulse. The corresponding Keldysh parameter is 6. Figure 2(a) compares the electric field of a chirp-free pulse with those having a positive and a negative chirp.

In Fig. 2(b), we compare the PES of H by laser pulses with three different chirp rates ξ. For the chirp-free pulse, the PES consists of a series of ATI peaks equally separated by the photon energy (i.e., 3.1 eV). Clearly, the chirp rate ξ very strongly affects the PES, which can be attributed to the different contributions of the excited bound states for the different chirp rates. In Fig. 2(c), we show the total population of 39 excited bound states of H by laser pulses with three different chirp rates.

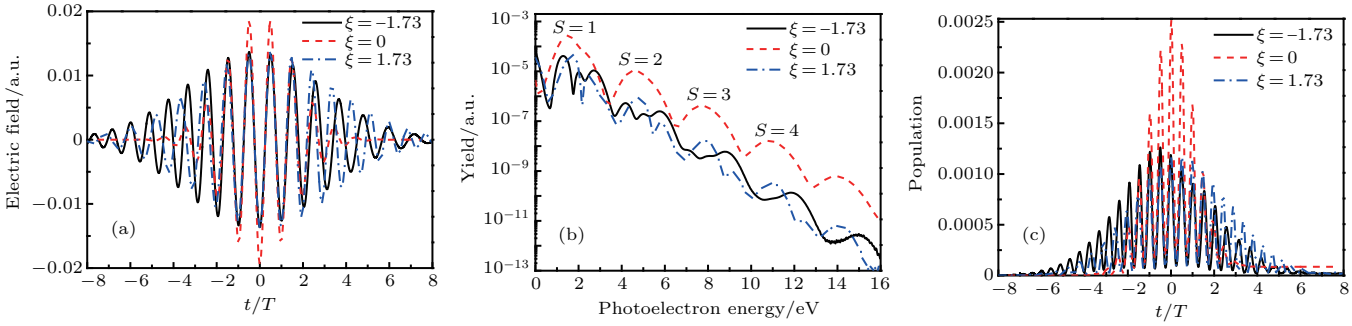


Fig. 2. (color online) Chirp dependence of (a) the electric field of laser pulses; (b) photoelectron energy spectra of H; and (c) total population of excited bound states of H. We consider three different chirp rates, i.e., $\xi = -1.73$ (solid), $\xi = 0$ (dashed), and $\xi = 1.73$ (dot-dashed).

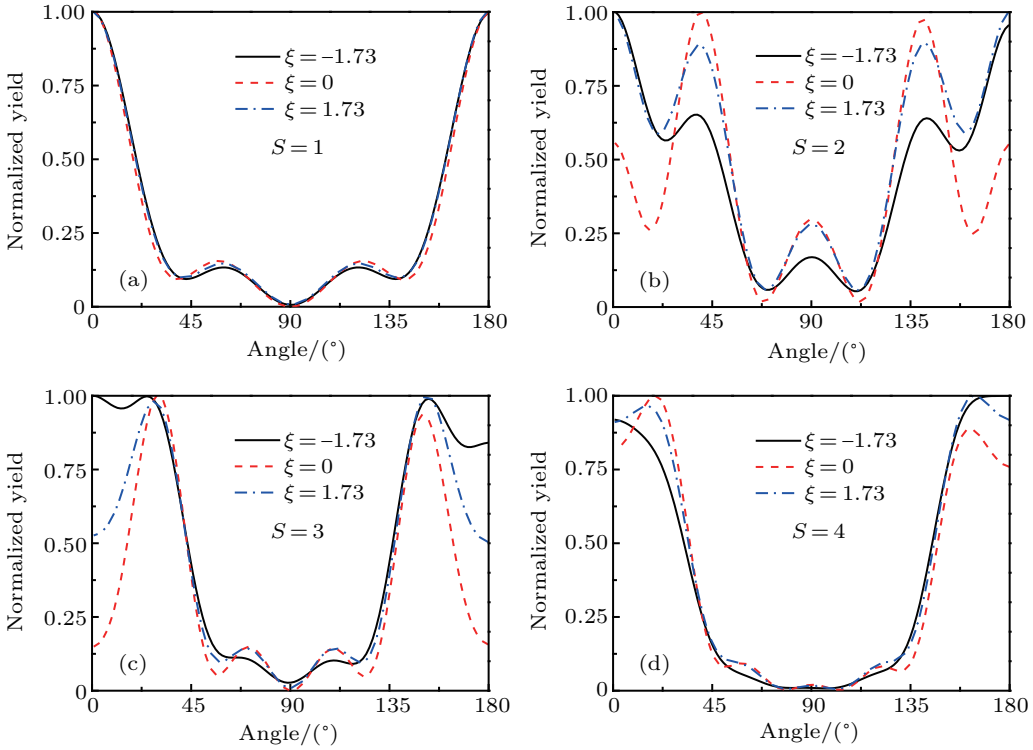


Fig. 3. (color online) Photoelectron angular distributions of H at different photoelectron energies by the chirped pulses with three chirp rates: $\xi = -1.73$ (solid), $\xi = 0$ (dashed), and $\xi = 1.73$ (dot-dashed). The orders of the ATI peaks are (a) $S = 1$, (b) $S = 2$, (c) $S = 3$, and (d) $S = 4$, as labeled in Fig. 2(b). The laser parameters are the same as those in Fig. 2.

One can see that the instantaneous population of H for the chirp-free pulse is quite different from that using a positive (or negative) chirped pulse. Even for the same $|\xi|$, the instantaneous populations are still very different for $\pm\xi$. It indicates that the excitation dynamics of the excited bound states are quite different due to the different time-dependent instantaneous frequency components for the unchirped and chirped laser pulses. This is the reason why the PES is different for the three cases of $\xi = -1.73$, $\xi = 0$, and $\xi = 1.73$.

The PADs are calculated by integrating over one-photon energy (i.e., 3.1 eV) around several ATI peaks labeled as $S = 1$, 2, 3, and 4 in Fig. 2(b). We mention that the same energy ranges are used to calculate the PADs both for the unchirped and chirped laser pulses. For simplicity, all the PADs and the 2D momentum spectra are normalized to 1.0 at the peak throughout this paper unless otherwise stated. Clearly, the PADs show a chirp dependence especially for $S = 2$ and 3 as shown in Fig. 3.

For the chirped laser pulses, the low-energy 2D momentum spectra have more complex structures than that of the chirp-free case as shown in Fig. 4. We can see the sidebands in the first ATI peak and that the peak is shifted toward the smaller (larger) momentum for the negative (positive) chirped pulse compared with that of the unchirped laser case. The reason is that the electron can be ionized by simultaneously absorbing 5 photons at least, which corresponds to the first ATI peak for the unchirped pulse. However, the situation is quite different for the chirped laser case. The active electron can simultaneously absorb 5 photons whose instantaneous frequency is higher (or lower) than the unchirped laser frequency (i.e., 3.1 eV), which causes the sideband structures and the slight shift of the first ATI peak. On the other hand, the momentum spectra far below the first ATI peak exhibit very strong chirp dependence. It indicates that the 4-photon channel is closed for the unchirped laser but opened for the chirped pulses under the present chirp rates.

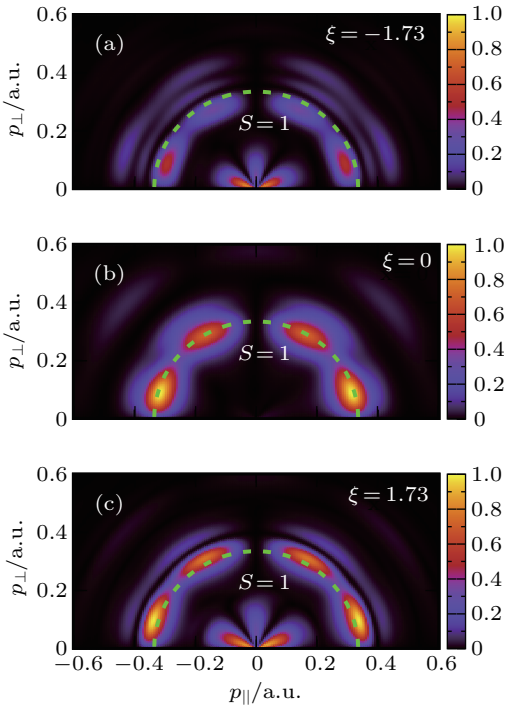


Fig. 4. (color online) Low-energy photoelectron 2D momentum distributions of H in the multiphoton ionization region by the chirped pulse with three different chirp rates: (a) $\xi = -1.73$, (b) $\xi = 0$, and (c) $\xi = 1.73$. The laser parameters are the same as those in Fig. 2.

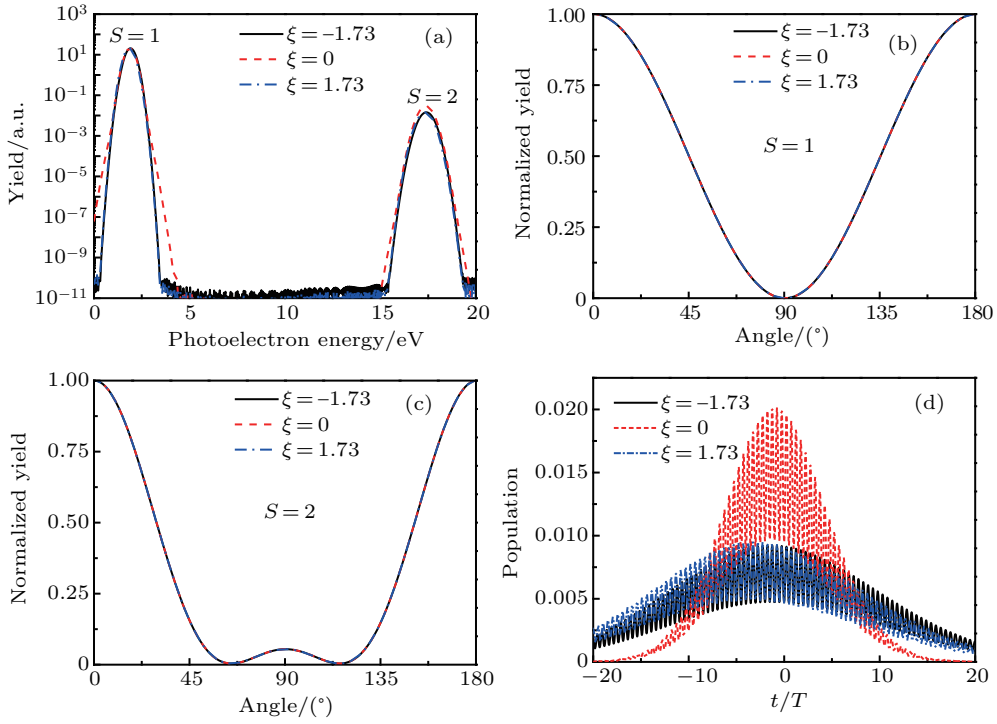


Fig. 5. (color online) Chirp dependence of (a) photoelectron energy spectra; (b), (c) photoelectron angular distributions at different photoelectron energies; and (d) total population of excited bound states of H. The orders of the ATI peaks are (b) $S = 1$ and (c) $S = 2$ as labeled in (a). We consider three different chirp rates, i.e., $\xi = -1.73$ (solid), $\xi = 0$ (dashed), and $\xi = 1.73$ (dot-dashed). The single photon energy is 15.5 eV.

3.3. Single-photon ionization

To check the argument that the chirp dependence essentially comes from the intermediate bound states in Ref. [17], we consider a 5 fs laser pulse with a laser peak intensity of 7.9×10^{13} W/cm^2 and the central wavelength of 80 nm. The corresponding Keldysh parameter is 12. The single photon energy is 15.5 eV and thus the active electron in the ground state of H can be removed by absorbing a single photon. Figure 5(a) presents the photoelectron energy spectra of H for the laser pulses with three different chirp rates. In Figs. 5(b) and 5(c), we show the PADs corresponding to the two ATI peaks (i.e., $S=1,2$ labeled in Fig. 5(a)). The 2D momentum spectra of H are also given in Fig. 6. Clearly, the photoelectron energy spectra, the PADs, and the 2D momentum spectra have no chirp dependence in the single-photon ionization region, which is consistent with the Na atom case in Ref. [17]. This is expected because the electron in the initial ground state can be directly released into the continuum state by a single-photon process and thus the intermediate excited bound states play a less important role, although the electron is capable of populating in the excited states (see Fig. 5(d)).

3.4. Tunneling ionization

Finally, we study how the tunneling ionization depends on the chirp rate of the laser pulses. It is known that the active electron in the ground state of an atom can tunnel through the potential barrier and thus the excited bound states would play a minor role in the tunneling ionization, while the tunneling process is dominantly affected by the laser field. In our simulations, we use a 5 fs laser pulse with central wavelength of 800 nm and peak intensity of 3.16×10^{14} W/cm^2. The corresponding Keldysh parameter is 0.6.

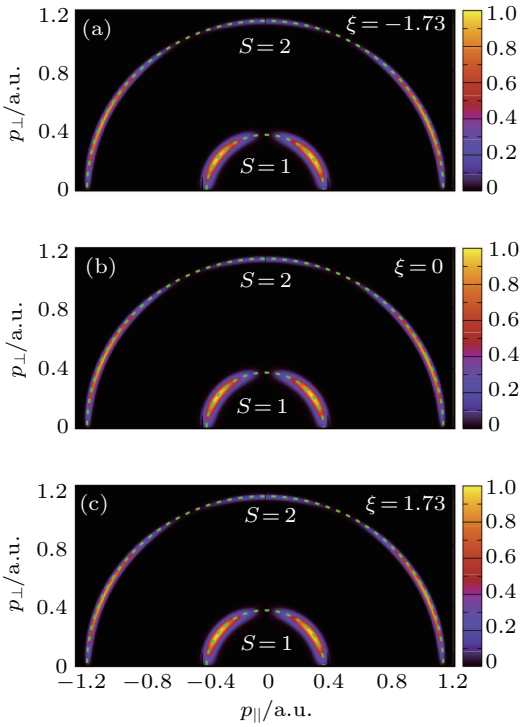


Fig. 6. (color online) Low-energy photoelectron 2D momentum distributions from single-photon ionization by the laser pulses for three different chirp rates: (a) $\xi=-1.73$, (b) $\xi=0$, and (c) $\xi=1.73$. To make both ATI peaks (i.e., $S=1$ and 2) visible, we renormalize the $S=2$ with another normalization factor. The laser parameters are the same as those in Fig. 5.

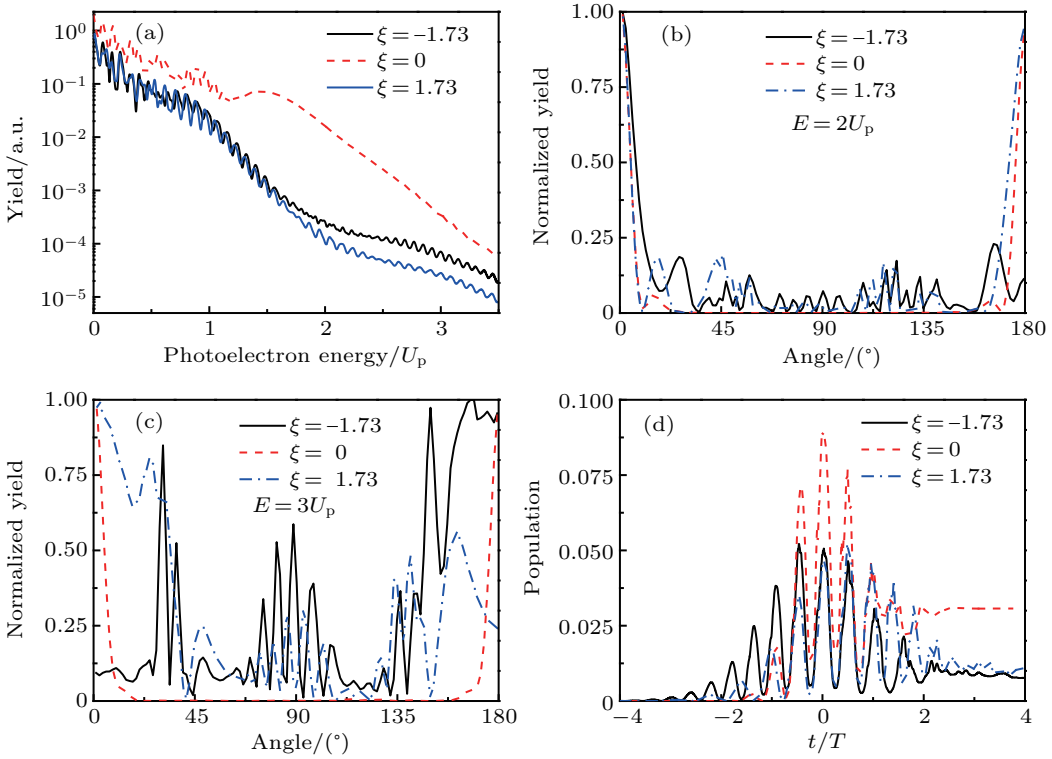


Fig. 7. (color online) Chirp dependence of (a) photoelectron energy spectra; (b), (c) photoelectron angular distributions at different photoelectron energies of $E=2U_p$ and $E=3U_p$, respectively; (d) total population of excited bound states of H. We consider three different chirp rates, i.e.,, $\xi=-1.73$ (solid), $\xi=0$ (dashed), and $\xi=1.73$ (dot-dashed).

Figure 7(a) demonstrates the photoelectron energy spectra of H by laser pulses with three different chirp rates in the tunneling ionization region. We can see that the ionization yield by the chirp-free laser pulse is larger than that from the chirped laser case. Even for the same $|\xi|$, the structures of the photoelectron energy spectra are still very different for $\pm\xi$. In Figs. 7(b) and 7(c), we show a very clear chirp dependence of the normalized PADs at energies of $2U_p$ and $3U_p$, respectively. One can see that the electron tunnels dominantly along the laser's polarization axis for the unchirped pulse as expected, while the off-axis tunneling ionization can also happen for the chirped pulses because its laser peak intensity reduces 2 times with respect to that of the unchirped pulse. The time-dependent total population of all the excited states is also presented in Fig. 7(d). It is also possible that the electron is firstly excited to some intermediate bound states and then tunnels through the potential barrier. In this case, the chirp dependence of the PADs should be partially attributed to the excited states.

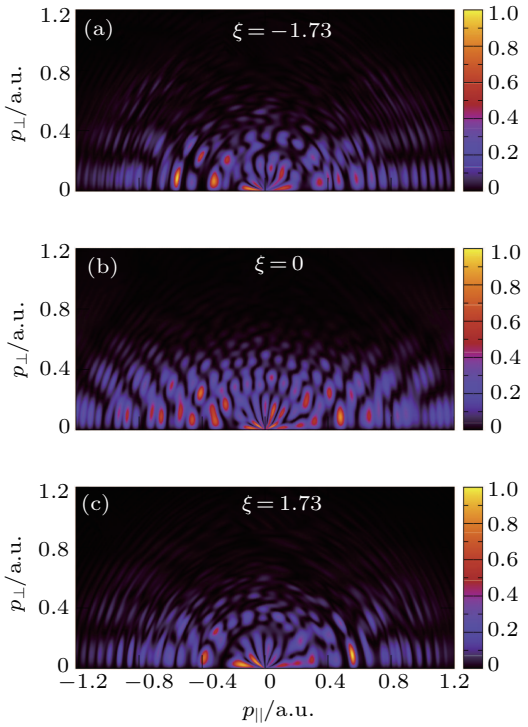


Fig. 8. (color online) Low-energy photoelectron 2D momentum distributions of H in the tunneling ionization region by a 5 fs laser pulse for three different chirp rates: (a) $\xi = -1.73$, (b) $\xi = 0$, and (c) $\xi = 1.73$.

Figure 8 presents the low-energy 2D momentum spectra of H by laser pulses with three different chirp rates. The momentum spectra exhibit a very clear chirp dependence. We can see that the very low-energy momentum spectra demonstrate ubiquitous fanlike structures both for the unchirped and chirped pulses. At the momentum $p = 0.077$ a.u., the dominant angular momentum is $L = 6$ (5) for the unchirped (chirped) pulses. Thus there are seven (six) peaks for the unchirped (chirped) pulses. Furthermore, the electrons tunnel preferably along the polarization direction of the laser fields in the tunneling ionization region for the unchirped laser, while the tunneling ionization away from the laser's polarization axis is enhanced significantly for the chirped pulses.

4. Conclusion

We theoretically study the chirp dependence of the ATI ionization processes of the hydrogen atom in an intense laser field by solving the TDSE. By comparing the energy spectra, the 2D momentum spectra, and the angular distributions of photoelectrons for the laser pulses with different chirp rates, we show a very clear chirp dependence both in the multiphoton and tunneling ionization processes, but no chirp dependence in the single-photon ionization. We also confirm that the chirp dependence in the multiphoton ionization based ATI can be attributed to the different excitation dynamics of intermediate bound states. In the single-photon and tunneling ionization regimes, the electron can be removed directly from the ground state and thus the excited states may not be very important. It indicates that the chirp dependence in the tunneling ionization based ATI processes is mainly due to the laser pulses with different chirp rates. Unfortunately, there is little experimental data available to examine these theoretical results, as far as we know.

References

[1] Agostini P, Fabre F, Mainfray G and Petite G 1979 *Phys. Rev. Lett.* **42** 1127
[2] Paulus G G, Nicklich W, Xu H, Lambropoulos P and Walther H 1994 *Phys. Rev. Lett.* **72** 2851
[3] Huismans Y, Rouzée A, Gijsbertsen A, Jungmann J H, Smolkowska A S, Logman P S W M, Lépine F, Cauchy C, Zamith S, Marchenko T, Bakker J M, Berden G, Redlich B, van der Meer A F G, Muller H G, Vermin W, Schafer K J, Spanner M, Ivanov M Yu, Smirnova O, Bauer D, Popruzhenko S V and Vrakking M J J 2011 *Science* **331** 61
[4] Blaga C I, Catoire F, Colosimo P, Paulus G G, Muller H G, Agostini P and DiMauro L F 2009 *Nat. Phys.* **5** 335
[5] Quan W, Lin Z, Wu M, Kang H, Liu H, Liu X, Chen J, Liu J, He X T, Chen S G, Xiong H, Guo L, Xu H, Fu Y, Cheng Y and Xu Z Z 2009 *Phys. Rev. Lett.* **103** 093001
[6] Wu C Y, Yang Y D, Liu Y Q, Gong Q H, Wu M, Liu X, Hao X L, Li W D, He X T and Chen J 2012 *Phys. Rev. Lett.* **109** 043001
[7] Guo L, Han S S, Liu X, Cheng Y, Xu Z Z, Fan J, Chen J, Chen S G, Becker W, Blaga C I, DiChiara A D, Sistrunk E, Agostini P and DiMauro L F 2013 *Phys. Rev. Lett.* **110** 013001
[8] Liu H, Liu Y Q, Fu L B, Xin G, Ye D, Liu J, He X T, Yang Y, Liu X, Deng Y, Wu C Y and Gong Q H 2012 *Phys. Rev. Lett.* **109** 093001
[9] Becker W, Grasbon F, Kopold R, Milošević D B, Paulus G G and Walther H 2002 *Adv. At. Mol. Opt. Phys.* **48** 35
[10] Milošević D B, Paulus G G, Bauer D and Becker W 2006 *J. Phys. B* **39** R203
[11] Chen Z, Le A T, Morishita T and Lin C D 2009 *Phys. Rev. A* **79** 033409
[12] Muller H G and Kooiman F C 1998 *Phys. Rev. Lett.* **81** 1207
[13] Murakami M, Zhang G P and Chu S I 2017 *Phys. Rev. A* **95** 053419
[14] Morishita T, Le A T, Chen Z and Lin C D 2008 *Phys. Rev. Lett.* **100** 013903
[15] Frolov M V, Knyazeva D V, Manakov N L, Geng J W, Peng L Y and Starace A F 2014 *Phys. Rev. A* **89** 063419
[16] Wang C L, Sun R P, Chen Y J, Gong C, Lai X Y, Kang H P, Quan W and Liu X J 2014 *Chin. Phys. Lett.* **31** 063202
[17] Nakajima T 2007 *Phys. Rev. A* **75** 053409
[18] Laulan S, Ba H S and Barmaki S 2014 *Can. J. Phys.* **92** 194
[19] Xiang Y, Niu Y and Gong S 2009 *Phys. Rev. A* **80** 023423

[20] Peng L Y, Tan F, Gong Q H, Pronin E A and Starace A F 2009 *Phys. Rev. A* **80** 013407
[21] Tan F, Peng L Y and Gong Q H 2009 *Chin. Phys. B* **18** 4807
[22] Pronin E A, Starace A F and Peng L Y 2011 *Phys. Rev. A* **84** 013417
[23] Brif C, Chakrabarti R and Rabitz H 2010 *New. J. Phys.* **12** 075008
[24] Varjú K, Mairesse Y, Carré B, Gaarde M B, Johnsson P, Kazamias S, López-Martens R, Mauritsson J, Schafer K J, Balcou Ph, L'Huillier A and Salières P 2005 *J. Mod. Opt.* **52** 379
[25] Chang Z, Rundquist A, Wang H, Christov I, Kapteyn H C and Murnane M M 1998 *Phys. Rev. A* **58** R30
[26] Lee D G, Kim J H, Hong K H and Nam C H 2001 *Phys. Rev. Lett.* **87** 243902
[27] Carrera J J and Chu S I 2007 *Phys. Rev. A* **75** 033807
[28] Zhao S F, Zhou X X, Li P C and Chen Z 2008 *Phys. Rev. A* **78** 063404
[29] Pan Y, Zhao S F and Zhou X X 2013 *Phys. Rev. A* **87** 035805
[30] Keldysh L V 1965 *Sov. Phys. JETP* **20** 1307
[31] Harris D O, Engerholm G G and Gwinn W D 1965 *J. Chem. Phys.* **43** 1515
[32] Dickinson A S and Certain P R 1968 *J. Chem. Phys.* **49** 4209
[33] Light J C and Walker R B 1976 *J. Chem. Phys.* **65** 4272
[34] Tong X M and Chu S I 1997 *Chem. Phys.* **217** 119
[35] Yudin G L, Bandrauk A D and Corkum P B 2006 *Phys. Rev. Lett.* **96** 063002
[36] Sun C P, Zhao S F, Chen J H and Zhou X X 2011 *Chin. Phys. B* **20** 113201